Water quality changes in acid mine drainage streams in Gangneung, Korea, 10 years after treatment with limestone

Moo Joon Shim[1], Byung Young Choi[2], Giehyeon Lee[3], Yun Ho Hwang[1],
Jung-Seok Yang[1], Edward J. O'Loughlin[4], and Man Jae Kwon[1*]

[1] Korea Institute of Science and Technology, Gangneung, KOREA
[2] Korea Institute of Geoscience and Mineral Resources, Daejeon, KOREA
[3] Earth System Sciences, Yonsei University, Seoul, KOREA
[4] Biosciences Division, Argonne National Laboratory, Argonne, USA

*Corresponding Author: Korea Institute of Science and Technology, Gangneung, KOREA, 679 Saimdangro, Gangneung, Gangwon-do, 210-340, Korea, Phone: +82-33-650-3705; Fax: +82-33-650-3729; mkwon@kist.re.kr

A manuscript submitted to *Journal of Geochemical Exploration*

May, 2015

ABSTRACT

To determine the long-term effectiveness of the limestone treatment for acid mine drainage (AMD) in Gangneung, Korea, we investigated the elemental distribution in streams impacted by AMD and compared the results of previous studies before and approximately 10 years after the addition of limestone. Addition of limestone in 1999 lead to a pH increase in 2008, and with the exception of Ca, the elemental concentrations (e.g., Fe, Mn, Mg, Sr, Ni, Zn, S) in the streams decreased. The pH was 2.5-3 before addition of limestone and remained stable at around 4.5-5 from 2008 to 2011, suggesting the reactivity of the added limestone was diminished and that an alternative approach is needed to increase the pH up to circumneutral range and maintain effective long-term treatment. To identify the processes causing the decrease in the elemental concentrations, we also examined the spatial (approximately 7 km) distribution over three different types of streams affected by the AMD. The elemental distribution was mainly controlled by physicochemical processes including redox reactions, dilution on mixing, and co-precipitation/adsorption with Fe (hydr)oxides.

Keywords: Acid mine drainage; Metals; Sulfate; Limestone treatment

1. Introduction

Acid mine drainage (AMD) has been extensively studied due to its negative impacts on aquatic environments. AMD is characterized by low pH and high concentrations of sulfate (SO_4^{2-}), Fe, Al, and other heavy metals (Equeenuddin et al., 2010; Kim and Chon, 2001; Kleinmann et al., 1981). In general, AMD is generated by the oxidation of pyrite (FeS_2) from coal mines when pyrite is exposed to air and water (Kim and Chon, 2001). During the oxidation of pyrite, SO_4^{2-}, ferrous iron (Fe^{2+}), and hydrogen ions (H^+) are released, causing a decrease in pH. This acidic water formed by the oxidation of pyrite is corrosive and causes the leaching of metals (e.g., Al) from native rocks (Sullivan and Yelton, 1988; Tabaksblat, 2002). In addition, the oxidation of ferrous iron to ferric iron (Fe^{3+}) can lead to precipitation of Fe- and Al-(hydr)oxides or hydroxysulfate (Heikkinen and Räisänen, 2008; Yu and Heo, 2001) and removal of trace metals by adsorption on and/or co-precipitation with these precipitates (Benjamin, 1983; Johnson, 1986; Stumm and Sulzberger, 1992). Subsequently, desorption and dissolution of these precipitates may release these metals into the water column leading to downstream contamination (Butler et al., 2009). Thus, solid phases of Fe and Al can play important roles in the distribution and/or speciation of trace metals.

Abandoned mines are a major pollution concern in Korea as they are distributed all over the country and drainage from abandoned mine has severely deteriorated local water quality. Among the many AMD sites, Young Dong (YD) AMD discharge (up to 5000 $m^3\ d^{-1}$) to surrounding areas is one of the most serious environmental concerns in Korea (Wildeman et al., 2008). In addition, the local environments of this area are complex and dynamic, with the stream waters impacted by two abandoned coal mines and one non-impacted stream. Therefore, investigation of the transport and fate of major and trace metals needs to be considered in the context of these dynamic systems. Several past studies focused on the general impacts of AMD on geochemical characteristics of streams receiving AMD water (YD stream) and Imgok Creek(IC) (Fig. 1) (Chon et al., 1999; Kim and Chon, 2001; Lee et al., 2012; Woo et al., 2012; Yu and Heo, 2001; Yu et al., 1999; Yu, 1998).

After cessation of mining operations in 1995, limestone (and/or dolostone) was added in the

adit in 1999 (Wildeman et al., 2008) to reduce the acidity and to increase the pH and alkalinity of the AMD (Cravotta, 2003; Cravotta and Trahan, 1999; Hedin et al., 1994). Although several technologies (e.g., anoxic limestone drains, aerobic/anaerobic wetlands, permeable reactive barriers, and sulfidogenic bioreactors) were developed for AMD treatments (Fripp et al., 2000; Genty et al., 2012; Johnson and Hallberg, 2005), addition of limestone to AMD is known to be relatively simple and efficient for raising pH, accelerating the rate of oxidation of ferrous iron, and promoting precipitation of metals present in solution (Johnson and Hallberg, 2005). However, after the limestone addition, the effectiveness of this treatment for controlling YD AMD was not regularly monitored until 2008 when the Colorado School of Mines and the Mine Reclamation Corporation (MIRECO) co-assessed the impact of YD AMD on YD stream and IC (Lee et al., 2012). As such, effective treatment of the AMD by the added limestone was assumed for many years. No study attempted to evaluate changes in major and minor elemental distribution in the impacted areas. In addition, no study has shown whether large-scale limestone treatment resulted in increased alkalinity and metal removal in streams impacted by coal mines.

The objectives of the current study are to examine 1) the long-term changes in metal concentrations before and after limestone treatment by comparing our results with previous published data (1996-1997, 2008, and 2009) in YD AMD and these complex and dynamic streams and 2) the spatial variation of major and minor elements caused by a variety of physicochemical processes (i.e., mixing, dilution, redox reactions, dissolution, and precipitation). This study will help determine the geochemical behavior of trace and major elements, as well as clarify the factors controlling major and trace metals in the AMD and impacted streams. In addition, this study will allow us to assess the effectiveness of limestone treatment for increasing pH and metal removal.

2. Materials and methods

2.1 Study area and sampling

The Young Dong (37° 39′ 00″ N, 129° 00′ 00″ E) and Young Jin (37° 41′ 40″ N, 129° 56′ 30″

E,) coal mines are located in the Gangneung coal field in Korea (Fig. 1) and are well known for discharging enormous amounts of AMD (up to 5000 m^3 d^{-1}) to local areas (Wildeman et al., 2008). YD AMD flows into the YD stream and discharges into IC. Sampling stations were selected at five distinct water systems, which were determined by the geographical location of the AMD and streams (Fig. 1). General properties of five water systems are shown in Table 1.

Stream I represents the leachate (sky blue) and the YD stream (red), including stations 1, 2, 8, 9, 10, 11, 12, and 13 (Fig. 1). A rock pile was dug out to make another mine head for the YD coal mine in the upper part of stream I. The waters from stations 1 and 2 are comprised of leachates resulting from the interaction of rain water with the rock pile that discharge into YD stream. Stream II (green) waters are from the Young Jin mine, and include stations 3, 4, 5, 6, and 7. YD stream (red) receives stream II waters at station 10, and is characterized by a combination of waters from stream II and a mine head of YD discharging AMD (Fig. 1). Due to its location at the head of the YD stream, station 8 was used as a proxy for samples representing YD AMD. Station 9 was connected directly to station 8 with a tube-type plastic channel as part of the pilot-scale tests (active and semi-active treatment systems) for a future AMD treatment application by MIRECO, S. Korea. Therefore, the water quality from station 9 is similar to that of station 8. Stream III is composed of upstream of IC (dark blue) and downstream of IC (yellow). Upstream of IC (dark blue) is a non-AMD-impacted stream that converges with waters from the YD stream (red).

Water samples were collected from 22 stations and 20 stations in August and October, 2011, respectively. Two water samples from stations 16 and 17 were not collected due to the lack of water at these locations in October 2011. Surface water samples were manually collected (with plastic gloves) using acid-washed polyethylene bottles. Water samples for cation and anion analysis were filtered in the field using 0.45 μm cellulose membrane filters. Water samples for major and trace elements analysis were acidified to pH < 2 by adding concentrated HNO_3 to 50 mL of samples in the field. Solid precipitates at station 8 and 18 were also collected for mineralogical analysis at the same time as the water samples using stainless spatulas. All water and solid samples were stored on ice during transport

to the lab. The acidified samples were kept at room temperature until analysis, and the samples for anion analysis were kept under refrigeration until analysis.

Pyrite oxidation (biological and abiotic) leads to dissolved sulfate in AMD (Balci et al., 2007; Taylor and Nordstrom, 1984). Thus, the comparison of sulfur isotope ratios between dissolved sulfate and pyrite can trace the source of dissolved sulfate present in AMD. Sulfur isotope ratios ($\delta^{34}S$) of dissolved sulfate were also analyzed for selected samples (i.e., stations 1, 5, 8, 10, and 18) collected in August 2011. After lowering the pH of the sample solutions to 3-4 using concentrated HCl, $BaCl_2 \cdot 2H_2O$ was added to the filtered water sample to precipitate sulfate as $BaSO_4$. Precipitated $BaSO_4$ samples were collected using 0.45 μm cellulose membrane filters, and subsequently washed thoroughly with deionized water to remove Cl^- from the precipitates. The precipitates were then dried at room temperature.

2.2 Sample analysis

Electrical conductivity (EC) and pH were measured on site using a pH/EC meter (Thermo scientific, Orion Star A325), calibrated with certified standards. The concentrations of major and minor elements (Al, Fe, Mn, Mg, Ca, Sr, Li, Na, K, Co, Ni, Cu, Zn and Pb) were determined using an inductively coupled plasma-optical emission spectrometer (ICP-OES, Varian) using external standards for calibration. The lower limit of detection (LOD; mg L^{-1}) and the limit of quantification (LOQ; mg L^{-1}) of major and minor elements were 0.030 and 0.100 for Al, 0.003 and 0.009 for Ca, 0.001 and 0.002 for Co, 0.001 and 0.003 for Cu, 0.036 and 0.109 for Fe, 0.003 and 0.010 for K, 0.007 and 0.022 for Mg, 0.000 and 0.001 for Mn, 0.001 and 0.004 for Na, 0.003 and 0.010 for Ni, 0.006 and 0.022 for Pb, 0.001 and 0.002 for Zn, respectively. Acidity due to metals was calculated using the equation from Kirby and Cravotta (Kirby and Cravotta III, 2005): $Acidity_{computed}$ (mg L^{-1} $CaCO_3$) = 50 ($10^{(3-pH)}$ + $2C_{Fe}/55.8$ + $2C_{Mn}/54.9$ + $3C_{Al}/27.0$) where C_{Fe}, C_{Mn}, and C_{Al} are Fe, Mn, and Al concentrations, respectively. Sulfur was analyzed by ICP-OES and converted to sulfate by multiplying the sulfur concentrations by 3 (Lee et al., 2012). The concentration of aqueous Fe(II) was determined by using the ferrozine assay (Stookey,

148 1970). Briefly, 1 mL of HEPES (50 mM)-buffered ferrozine reagent (Sørensen, 1982) was added to
149 0.05 mL of sample, and the Fe(II) concentration was measured at 562 nm with a spectrophotometer
150 with a detection limit of 0.7 mg Fe(II) L^{-1}. To determine sulfur isotope ratios of sulfate, the dried $BaSO_4$
151 samples were converted to SO_2 in an elemental analyzer, and analyzed by isotope ratio mass
152 spectrometry in continuous-flow mode at Korea Basic Science Institute (Korea). Samples for powder
153 x-ray diffraction (pXRD) analysis were prepared by passing approximately 20 mL of suspension
154 through Nylon filters (45 mm, 0.45 μm). The pXRD data were collected with an X'Pert Pro MPD X-
155 ray diffractometer with Ni-filtered Cu Kα radiation. The samples were scanned between 10° and 80° 2θ
156 at a speed of 2.5° 2θ min^{-1}. Chemical compositions of precipitates were analyzed using wavelength
157 dispersive X-ray fluorescence (WD-XRF) spectrometry at Korea Basic Science Institute.
158 The precipitation of Fe and Al in conjunction with chemical analysis data of stream waters
159 was computed by the geochemical program PHREEQC version 3 (Parkhurst and Appelo, 2013) using
160 the database of thermoddem.dat (Blanc et al., 2012)(Table S1). Each mineral phase can be precipitated
161 when its saturation index (SI) > 0 was reached or dissolved completely when SI < 0.
162
163 **3. Results and discussion**
164 **3.1 General water quality and mineralogical characteristics of precipitates**
165 The results of sulfate, EC, $acidity_{computed}$, and pH, and EC measured in August and October
166 2011 are shown in Figure 2 and Table S2. Although stream discharge was not determined in this study,
167 the precipitation data suggested that the stream discharge in August was greater than that in October
168 (data not shown). However, sulfate, EC, $acidity_{computed}$ and pH at most stations in August were similar
169 to those in October (Fig. 2). Most of elements also showed little temporal difference.
170 Although the pH did not show a temporal trend, it was dynamic spatially. The pH of waters
171 from streams I and II was generally low, ranging from 3.2 to 5.1. The pH of downstream waters of IC
172 was higher due to the inclusion of circumneutral (pH 6.4 to 8.1) upstream IC waters (Fig. 2).
173 The EC of leachate (stations 1 and 2) was also low, but increased markedly when this water

joined with the YD stream at station 8 (Fig. 2). This is because the water at station 8 was from a mine adit of YD AMD with high dissolved ions, particularly sulfate and iron (Chon et al., 1999; Kim and Chon, 2001; Yu and Heo, 2001; Yu et al., 1999). In spite of the relatively long distance (approximately 300 m) between station 8 and 9, the EC at these stations was similar because of the direct connection between these stations as described in the previous section. This high EC decreased during mixing of stream II, but EC rebounded and stabilized. The EC sharply decreased again when the YD stream mixed with waters from upstream IC, and remained low along downstream IC. The spatial distribution of sulfate showed a similar pattern to EC (Fig. 2) which was not surprising because sulfate was the most abundant anion in waters collected in this area.

The low pH and high sulfate concentrations of waters at station 8 and 9 are consistent with their direct discharge from the adit of YD mine where there has been extensive oxidation of pyrite. In fact, the $\delta^{34}S$ (-0.50‰) of dissolved sulfate at station 8 of the current study was similar to the $\delta^{34}S$ (1.1-1.8‰) of dissolved sulfate and the $\delta^{34}S$ (0.0 ~ 1.6‰) of the pyrite around YD coal mine (Yu and Coleman, 2000). The $\delta^{34}S$ of dissolved sulfate at stations 1, 5, 10, and 18 was 0.17, -0.69, -0.61, and -0.69‰, respectively. Little to no fractionation of sulfur isotopes during pyrite oxidation suggests that the $\delta^{34}S$ of dissolved sulfate in this area can be utilized to track the acid source. Fe^{2+} from the pyrite is oxidized to Fe^{3+}, and the oxidized Fe and solubilized Al can be precipitated as Fe and Al oxides or hydroxysulfate (Heikkinen and Räisänen, 2008; Yu and Heo, 2001). Yellow/red brownish and whitish precipitates were observed in YD stream and downstream of IC during water collection (Fig. 1). XRD and/or XRF analysis indicated that the yellow/brownish precipitates at station 8 were goethite (α-FeOOH) and the whitish precipitates at station 18 were hydrobasaluminite or basaluminite ($Al_4(OH)_{10}SO_4$) depending on the extent of hydration (Fig. S1 and Table S3). The iron mineral phase identified near the adit of YD mine was different from the previous studies which reported ferrihydrite and schwertmannite ($Fe_8O_8(OH)_6SO_4$) (Chon et al., 1999; Kim and Chon, 2001; Yu and Heo, 2001). It is well known that ferrihydrite and goethite can be precipitated at circumneutral pH, while schwertmannite is the most common Fe phase precipitating between pH 3 and 4 (Bigham et al., 1996).

Thus, it is possible that the increase in pH (close to 5) due to the addition of limestone might affect the phase of the iron precipitates in the area. The SI calculation also supported that the waters at stations 8-13 were oversaturated (SI > 0) with respect to goethite, but were undersaturated (SI < 0) with respect to schwertmannite (Table S1).

3.2 Physicochemical processes affecting spatial distribution of major and trace elements

3.2.1 Fe, Mn, Mg, Ca, Sr, Li, Co, Ni, Zn, and Pb

The spatial distribution of Fe, Mn, Mg, Ca, Sr, Li, Co, Ni, Zn, and Pb (Fig 3A) was very similar with that of EC and sulfate (Fig. 2). Concentrations of these elements (Table S2) in leachates (stations 1 and 2) were low, but sharply increased at the YD stream. Increases in trace metals at stations 8 and 9 are likely the result of discharge from the YD mine adit. Concentrations of Ca and Mg were also higher at these stations most likely because of the dissolution of calcite ($CaCO_3$) and dolomite ($CaMg(CO_3)_2$) from the limestone and dolostone placed in the adit. Limestone and dolomite have been used to treat AMD by neutralizing the acidity of AMD and precipitation of metals (Cravotta, 2003; Cravotta and Trahan, 1999; Fripp, 2000; Genty et al., 2012; Hedin et al., 1994).

Elemental concentrations decreased at stations where YD stream water mixed with stream II (which had relatively low concentrations of Fe, Mn, Mg, Ca, Sr, Li, Co, Ni, Zn, and Pb). Waters from stream II originated from the Young Jin mine (Fig. 1), but Fe concentrations were relatively low compared those in the YD stream. The lower concentrations of Fe in waters from stream II are likely due to precipitation of Fe (as confirmed by visual inspection) during the longer transit of AMD from the head of Young Jin mine. The pH of stream II ranged between 3.4 and 4.9. Fe can be precipitated as schwertmannite and/or ferrihydrite even in water having pH values < 5 (Chon et al., 1999; Lee et al., 2002).

Concentrations of Fe were also very low in the leachates flowing into YD stream despite the relatively low pH. Given that yellow/red brownish precipitates were not observed at stations 1 and 2 (Fig. 1), runoff might react with rock piles leading to rapid oxidation of Fe^{2+} and precipitation of Fe^{3+}

226 in place. Unlike in the leachates and stream II, Fe concentrations were high at stations 8 and 9 due to
227 rapid discharge from the YD mine adit. The water that came out of the adit may have been deoxygenated
228 at the origin (below ground) and rapidly transported to the surface; as a result, the high dissolved Fe (as
229 Fe^{2+}) content relative to the waste rock piles was observed (Table S2). Thus, redox processes as well as
230 pH may have influenced the downstream behavior of the metals we monitored.
231 The concentrations of major and minor elements at stations 10, 11, 12, and 13 were relatively
232 constant until dilution by upstream waters of IC at station 18. The concentrations of these elements
233 gradually decreased in downstream IC. As stated above, several studies elucidated that Fe was removed
234 by mineral precipitation as ferrihydrite and schwertmannite ($Fe_8O_8(OH)_6SO_4$) in IC and YD stream
235 (Chon et al., 1999; Kim and Chon, 2001; Yu and Heo, 2001). It was also suggested that other metals
236 were removed by adsorption and/or co-precipitation with Fe and Al precipitates based on XRD and
237 chemical equilibrium calculation (Yu and Heo, 2001). XRD results indicated that stations 8 and 18
238 contained no crystalline metal precipitates except Fe phases (Fig. S1), and chemical equilibrium
239 calculation revealed that all YD stream and IC waters were undersaturated with respect to most of the
240 trace metal-bearing minerals considered (Table S1)(Yu and Heo, 2001). Therefore, adsorption and co-
241 precipitation have been suggested as important mechanisms to explain metal attenuation in streams
242 affected by AMD (Herr and Gray, 1996; Johnson, 1986; Kwong et al., 1997; Lee and Faure, 2007; Yu,
243 1996). The relationship between Fe and the other metals was significantly correlated (Fig. S2) when the
244 data from the leachates, the upstream waters of IC, and stream II were excluded (where no or little
245 yellowish or brownish precipitates were observed). This suggests that Mn, Mg, Ca, Sr, Li, Co, Ni, Zn,
246 and Pb may be adsorbed and/or co-precipitated with Fe precipitates in the YD stream and downstream
247 of IC.
248 On the other hand, various Mn oxides have been also known to adsorb trace metals (Adelson
249 et al., 2001; Brown et al., 2000; Fernex et al., 1992; Godfrey et al., 1994; Morford et al., 2005; Nameroff
250 et al., 2002), and precipitation of Mn (e.g., birnessite and manganite) can occur at pH > 7 in natural
251 waters contaminated with AMD (Lee et al., 2002). However, the pH values in YD stream and

downstream of IC were ≤ 5 and ≤ 7.3, respectively. In addition, XRF data indicated that Mn concentrations were much less than Fe and Al at stations 8 and 18 (Table S3) suggesting that Mn precipitates might not play significant roles in scavenging trace metals in this area.

3.2.2 Al and Cu

Al and Cu showed different spatial distributions (Fig. 3B) compared to the metals of the first group (Section 3.2.1). Concentrations of these two elements were highest in the leachates (stations 1 and 2) from the rock piles. The pH at stations 1 and 2 was also lowest (Table 2) and might promote the dissolution of aluminosilicate minerals as well as sulfide minerals, possibly copper sulfides among others. The range of pH (3.2 - 3.8) with high concentrations of Al is consistent with buffering as a result of aluminosilicate dissolution in localized low pH water due to sulfide oxidation within the rock pile (Ciccarelli et al., 2009; Mattson, 2009).

At station 8, Al concentrations noticeably decreased, likely due to the increase in pH resulting in significant precipitation of Al (Table S1 and S3). Al quickly decreased again at the confluence of the YD stream with upstream waters of IC (which have a relatively high pH) (Fig. 3B), where the pH increased above 5 leading to precipitation of solid phases of Al. In fact, whitish precipitates (possibly Al hydroxysulfate ($Al_4(OH)_{10}SO_4$) in the current and previous study (Yu and Heo, 2001)) were observed at or around the station 18 (Fig. 1 and Table S3).

Cu concentrations decreased at the confluence of the YD stream with upstream waters of IC, becoming almost non-detectable in downstream waters of IC. It is possible that the concentrations of Cu decreased simply by dilution on mixing with upstream waters of IC, which contained < 0.02 mg L^{-1} Cu. On the other hand, correlation between liquid phase Al and Cu concentrations was significant (r^2= 0.978 and 0.693 in August and October 2011, respectively). Therefore, the decrease in Cu concentrations (particularly in downstream in IC) was likely due to the removal by adsorption on and/or co-precipitation with Al solid phases. Cu did not show a significant correlation with Fe (data not shown), suggesting Cu might not be adsorbed and/or co-precipitated with Fe solid phases. This result was

different from other studies that reported Cu was strongly correlated with Fe and had a high affinity for Fe oxides (Butler et al., 2009; Kinniburgh et al., 1976). In contrast, this result is consistent with the study reporting Al oxide is more favored to adsorb Cu than Fe oxide (Caraballo et al., 2011; Karthikeyan et al., 1997). The study suggested that Cu can be significantly removed when co-precipitated with hydrous ferric oxides (HFO), but not so effectively removed by adsorption onto already formed HFO. If HFO was already formed prior to contact with Al rich streams, then adsorption might not be significant and co-precipitation/adsorption with hydrous aluminum oxides (HAO) more favorable.

3.3 Long-term variation of elemental distribution in YD and IC streams: comparison with past studies

Figure 4 shows the ranges of pH, cations, and sulfate in the YD stream determined in this and past studies (Chon et al., 1999; Lee et al., 2012; Woo et al., 2012; Yu and Heo, 2001). Chon et al. (1999) collected water samples on YD stream and IC in December 1996 and April 1997. Yu and Heo (2001) also collected water samples October 1996, and April and October 1997. After more than ten years, Lee et al. (2012) and Woo et al. (2012) collected and assessed water samples (including station 8) in March 2009 and March 2008, respectively, from YD stream and IC.

As stated previously, limestone was added to the adit of the YD mine to decrease the acidity of AMD waters. However, we were not able to find any studies verifying that the efficacy of this treatment. In addition, the lack of elemental concentration data immediately after the limestone addition makes it difficult to predict the performance of the limestone treatment after 10 years. In spite of these limitations, we compared major and minor elemental distributions measured before and after the limestone addition. The pH of YD stream before limestone addition (i.e., 1996 and 1997) was ~ 2.5-3 (Chon et al., 1999; Yu and Heo, 2001); however, the data after the addition (i.e., 2008 – 2011) showed a higher pH range (4-5) (Fig. 4). These data suggest that the increase in pH (2 → 4) from 1997 to 2009 was due to the reaction of AMD water with the limestone added in the adit.

Interestingly, calcium did not decrease much from the values of 1996-97 to 2008-2011 (Fig. 4)

304 suggesting that the limestone treatment was still working to some extent. The pH did not change
305 considerably from 2008/2009 to 2011, suggesting that the limestone buffering capacity remained the
306 same over this period. However, limestone (calcite) is known to control pH up to ~ 8.3 under
307 atmospheric CO_2 levels. In general, many calcite remediation systems raise the pH to 7 depending upon
308 CO_2 pressure and Ca concentration. Thus, the pH levels of ~ 4.5 - 5 in the YD stream suggest that the
309 neutralization capacity of limestone added is not enough to increase the pH to 7. Also, it is possible that
310 the diminished increase in pH might be due to the release of acid from the transformation of iron
311 oxides/hydroxysulfates, (e.g. schwertmannite) over time to goethite (Burton et al., 2008):

312 $$Fe_8O_8(OH)_{8-2x}(SO_4)_{x(s)} + \quad 2xH_2O \quad \rightarrow \quad 8FeOOH_{(s)} + xSO_4^{2-} + 2xH^+$$

313 The identification of goethite rather than schwertmannite at station 8 supports this possibility
314 (Fig. S1 and Table S1). In addition, limestone treatment can be inefficient when Fe concentrations are
315 high due to coating of limestone surfaces by Fe oxide precipitates that can inhibit reaction of limestone
316 with acidic mine water (Akcil and Koldas, 2006; Hammarstrom et al., 2005). Precipitation of gypsum
317 ($CaSO_4 \bullet H_2O$) is also known to passivate limestone (Hammarstrom et al., 2005), but the water at station
318 8 is undersaturated with respect to gypsum (Table S1). The results suggest that placement of greater
319 quantities of limestone or smaller sized material with more surface area and periodic
320 replacement/rejuvenation of the limestone is needed for long-term effectiveness in treating AMD (Fripp,
321 2000; Van Hille et al., 1999). Biological treatments can be an alternative to chemical treatments (e.g.,
322 limestone) to increase the pH of AMD. For instance, the pH increased from 2.8 to 6.2 during treatment
323 of AMD by sulfate-reducing bacteria in bench scale experiments (Bai et al., 2013). This method was
324 effective to remove both sulfate and metals as sulfate-reducing bacteria reduce sulfate to hydrogen
325 sulfide which then precipitates with metal ions as metal sulfides. Photosynthetic microorganisms can
326 also generate alkalinity by consuming bicarbonate and producing hydroxyl ions (Johnson and Hallberg,
327 2005) as demonstrated in a bench scale experiment using the alga *Spirulina* sp. to treat AMD, where
328 pH increased from 1.8 to over 7 (Van Hille et al., 1999). Thus, biological treatments in a successive
329 alkalinity-producing systems (SAP) process may be an option to increase pH and reduce sulfate and

metal levels, although it may not be adequate at the peak flows of 5000 m^3/day suggested for AMD in this system.

Except for Ca, the concentrations of elements in the current study and the study in 2008 and 2009 generally decreased compared to data collected in 1996-1997 mainly due to the increase in pH (Fig. 4). It is difficult to assess whether these changes were just due to different hydrological conditions because no data on stream hydrology and seasonal variations in water quality are available. However, monthly precipitation totals during this and past studies varied regardless of rainy or dry seasons; 139.3, 22.5, 49.6, 3.9, 117.3, 70.9, 121.2, and 64.8 mm in Oct 1996, Dec 1996, April 1997, Oct 1997, Mar 2008, Mar 2009, Aug 2011, and Oct 2011, respectively. Therefore, it is unlikely that the long-term decreases in metals and major ions were just because samples were taken during the rainy season.

The elemental distribution and pH ranges of IC in this and previous studies (Chon et al., 1999; Lee et al., 2012; Woo et al., 2012; Yu and Heo, 2001) are shown in Fig. 5. Similar to the results of YD stream, the pH in IC generally increased after limestone addition. The pH in IC was higher than in YD stream in both current and past studies. Except for the 1996-1997 study (Chon et al., 1999), pH reached up to 7 in downstream waters of IC. Interestingly the pH measured in 1996-1997 (before the limestone treatment) ranged from 2.6 to 7.0 (Yu and Heo, 2001) (Fig. 5). This suggests that the limestone treatment might not be the only factor to controlling the pH in downstream waters of IC, although addition of limestone has prevented the high fluctuation in pH in the IC with pH ranging from ~5 to 7 during 2008-2011 (in contrast, in 1996/97 the pH varied greatly from 2.6 to 7.0). Mixing and alkalinity addition by upstream waters of IC might be one of the major controlling factors for pH in downstream of IC. Most of the major and trace elements temporally decreased in IC compared to the study in 1996-1997 likely due to reduced metal loads from YD stream after the limestone treatment.

Regarding maximum contaminant levels (MCLs) of several contaminants measured in this study, the concentrations of Pb, Al, Fe, Mn, and SO_4^{2-} in YD stream are above the MCLs, while Fe and Mn in downstream IC exceeded the maximum contaminant levels (Table S2 and S4). These data suggest that the streams impacted by AMD require additional treatment and public attention.

4. Conclusion

YD AMD contributed to high concentrations of major and trace elements such as Ca, Mg, Fe, Mn, Co, Li, Ni, Pb, Sr, and Zn in the YD stream. However, most of the elements decreased except K and Na during water transport from the YD stream to IC. Physicochemical factors such as dilution by mixing, co-precipitation/adsorption, redox processes, and pH fluctuation were major controlling factors for the spatial distribution of major and trace elements in YD stream and IC.

Most of the elements analyzed in this study decreased in YD stream and IC after 1999 possibly due to the pH increase attributed to the limestone addition. Therefore, the limestone treatment was effective for reducing trace metal concentrations. However, pH was stable at around 4.5 - 5 from 2008 to 2011 in YD stream, implying that the limestone addition for YD AMD treatment increased the pH to 5 within 10 years, but did not increase pH after then and that the neutralization capacity of limestone added may have decreased leading to less than optimal performance.

The performance of the limestone treatment may be improved by placement of greater quantities of limestone (or more reactive limestone – i.e., smaller sized material with more surface area) as well as periodic replacement of the limestone to maintain reactivity. However, alternative treatment technologies may be needed for effective long-term environmental protection of this area. Moreover, although the major and trace metals we analyzed were significantly diminished by natural attenuation during water transport, the long-term monitoring of metal concentrations in IC requires further study.

Acknowledgements

We thank Mr. Woo Ram Lee for his assistance in field sampling. This work was supported by the KIST Institutional Program (Project No. 2Z04381) and by Korea Ministry of Environment as "The GAIA Project-2013000540005".

Supporting Information

382 Additional results for XRF and XRD analysis and saturation indices (10 pages, 3 Figures, 4 Tables).

383

384 **References**

385 Adelson JM, Helz GR, Miller CV. Reconstructing the rise of recent coastal anoxia; molybdenum in
386 Chesapeake Bay sediments. Geochimica et Cosmochimica Acta 2001; 65: 237-252.
387 Akcil A, Koldas S. Acid Mine Drainage (AMD): causes, treatment and case studies. Journal of Cleaner
388 Production 2006; 14: 1139-1145.
389 Bai H, Kang Y, Quan H, Han Y, Sun J, Feng Y. Treatment of acid mine drainage by sulfate reducing
390 bacteria with iron in bench scale runs. Bioresource Technology 2013; 128: 818-822.
391 Balci N, Shanks WC, Mayer B, Mandernack KW. Oxygen and sulfur isotope systematics of sulfate
392 produced by bacterial and abiotic oxidation of pyrite. Geochimica et Cosmochimica Acta,
393 2007; 71: 3796-3811.
394 Benjamin MM. Adsorption and surface precipitation of metals on amorphous iron oxyhydroxide.
395 Environmental Science & Technology 1983; 17: 686-692.
396 Bigham JM, Schwertmann U, Traina SJ, Winland RL, Wolf M. Schwertmannite and the chemical
397 modeling of iron in acid sulfate waters. Geochimica et Cosmochimica Acta 1996; 60: 2111-
398 2121.
399 Blanc, P., Lassin, A. and Piantone, P. (2012), THERMODDEM a database devoted to waste minerals,
400 BRGM, Orléans, France. http://thermoddem.brgm.fr
401 Brown ET, Le Callonnec L, German CR. Geochemical cycling of redox-sensitive metals in sediments
402 from lake malawi: a diagnostic paleotracer for episodic changes in mixing depth. Geochimica
403 et Cosmochimica Acta 2000; 64: 3515-3523.
404 Burton ED, Bush RT, Sullivan LA, Mitchell DRG. Schwertmannite transformation to goethite via the
405 Fe(II) pathway: Reaction rates and implications for iron–sulfide formation. Geochimica et
406 Cosmochimica Acta 2008; 72: 4551-4564.
407 Butler BA, Ranville JF, Ross PE. Spatial variations in the fate and transport of metals in a mining-
408 influenced stream, North Fork Clear Creek, Colorado. Science of the Total Environment 2009;
409 407: 6223-6234.

410 Caraballo MA, Macías F, Nieto JM, Castillo J, Quispe D, Ayora C. Hydrochemical performance and
411 mineralogical evolution of a dispersed alkaline substrate (DAS) remediating the highly
412 polluted acid mine drainage in the full-scale passive treatment of Mina Esperanza (SW Spain).
413 American Mineralogist 2011; 96: 1270-1277.
414 Chon HT, Kim JY, Choi SY. Hydrogeochemical Characteristics of Acid Mine Drainage around the
415 Abandoned Youngdong Coal Mine in Korea. Resource Geology 1999; 49: 113-120.
416 Ciccarelli JM, Weber PA, Stewart WS, Li J, Schumann R, Miller SD, et al. Estimation of long-term
417 silicate neutralisation of acid rock drainage. Proc. 8th Int. Conf. Acid Rock Drainage (8
418 ICARD), Skellefteå, Sweden, 2009, pp. 1-12.
419 Cravotta CA. Size and Performance of Anoxic Limestone Drains to Neutralize Acidic Mine Drainage.
420 Journal of Environmental Quality 2003; 32: 1277-1289.
421 Cravotta CAI, Trahan MK. Limestone drains to increase pH and remove dissolved metals from acidic
422 mine drainage. Applied Geochemistry 1999; 14: 581-606.
423 Equeenuddin SM, Tripathy S, Sahoo PK, Panigrahi MK. Hydrogeochemical characteristics of acid mine
424 drainage and water pollution at Makum Coalfield, India. Journal of Geochemical Exploration
425 2010; 105: 75-82.
426 Fernex F, Février G, Bénaïm J, Arnoux A. Copper, lead and zinc trapping in Mediterranean deep-sea
427 sediments: probable coprecipitation with Mn and Fe. Chemical Geology 1992; 98: 293-306.
428 Fripp J, Ziemkiewicz, PF, and Charkavorki, H. Acid mine drainage treatment, EMRRP Technical Notes
429 Collection (ERDC TN-EMRRP-SR-14). U.S. Army Engineer Research and Development
430 Center, Vicksburg, MS, 2000, pp. 1-7.
431 Johnson, DB, & Hallberg KB. Acid mine drainage remediation options: a review. Science of The Total
432 Environment 2005; 338: 3-14.
433 Genty T, Bussière B, Potvin R, Benzaazoua M, Zagury G. Dissolution of calcitic marble and dolomitic
434 rock in high iron concentrated acid mine drainage: application to anoxic limestone drains.
435 Environmental Earth Sciences 2012; 66: 2387-2401.

436 Godfrey LV, Mills R, Elderfield H, Gurvich E. Lead behaviour at the TAG hydrothermal vent field,
437 26°N, Mid-Atlantic Ridge. Marine Chemistry 1994; 46: 237-254.
438 Hammarstrom JM, Seal Ii RR, Meier AL, Kornfeld JM. Secondary sulfate minerals associated with
439 acid drainage in the eastern US: recycling of metals and acidity in surficial environments.
440 Chemical Geology 2005; 215: 407-431.
441 Hedin RS, Watzlaf GR, Nairn RW. Passive Treatment of Acid Mine Drainage with Limestone. Journal
442 of Environmental Quality 1994; 23: 1338-1345.
443 Heikkinen PM, Räisänen ML. Mineralogical and geochemical alteration of Hitura sulphide mine
444 tailings with emphasis on nickel mobility and retention. Journal of Geochemical Exploration
445 2008; 97: 1-20.
446 Herr C, Gray NF. Seasonal variation of metal contamination of riverine sediments below a copper and
447 sulphur mine in South-east Ireland. Water Science and Technology 1996; 33: 255-261.
448 Johnson CA. The regulation of trace element concentrations in river and estuarine waters contaminated
449 with acid mine drainage: The adsorption of Cu and Zn on amorphous Fe oxyhydroxides.
450 Geochimica et Cosmochimica Acta 1986; 50: 2433-2438.
451 Karthikeyan KG, Elliott HA, Cannon FS. Adsorption and Coprecipitation of Copper with the Hydrous
452 Oxides of Iron and Aluminum. Environmental Science & Technology 1997; 31: 2721-2725.
453 Kim J-Y, Chon H-T. Pollution of a water course impacted by acid mine drainage in the Imgok creek of
454 the Gangreung coal field, Korea. Applied Geochemistry 2001; 16: 1387-1396.
455 Kinniburgh DG, Jackson ML, Syers JK. Adsorption of Alkaline Earth, Transition, and Heavy Metal
456 Cations by Hydrous Oxide Gels of Iron and Aluminum1. Soil Science Society of America
457 Journal 1976; 40: 796-799.
458 Kirby CS, Cravotta III CA. Net alkalinity and net acidity 2: Practical considerations. Applied
459 Geochemistry 2005; 20: 1941-1964.
460 Kleinmann RLP, Crerar DA, Pacelli RR. Biogeochemistry of acid mine drainage and a method to
461 control acid formation. Journal Name: Min. Eng. (N.Y.); (United States); Journal Volume: 33:3

462 1981: Medium: X; Size: Pages: 300-305.
463 Kwong YTJ, Roots CF, Roach P, Kettley W. Post-mine metal transport and attenuation in the Keno Hill
464 mining district, central Yukon, Canada. Environmental Geology 1997; 30: 98-107.
465 Lee B-T, Ranville J, Wildeman T, Jang M, Shim Y, Ji W, et al. Assessment of Young Dong tributary and
466 Imgok Creek impacted by Young Dong coal mine, South Korea. Environmental Geochemistry
467 and Health 2012; 34: 95-103.
468 Lee G, Bigham JM, Faure G. Removal of trace metals by coprecipitation with Fe, Al and Mn from
469 natural waters contaminated with acid mine drainage in the Ducktown Mining District,
470 Tennessee. Applied Geochemistry 2002; 17: 569-581.
471 Lee G, Faure G. Processes Controlling Trace-Metal Transport in Surface Water Contaminated by Acid-
472 Mine Drainage in the Ducktown Mining District, Tennessee. Water, Air, and Soil Pollution
473 2007; 186: 221-232.
474 Mattson B. Assessing the availability and source of non-carbonate neutralisation potential by pre-
475 treatment of kinetic test samples. Proc. 8th Int. Conf. Acid Rock Drainage (8 ICARD),
476 Skellefteå, Sweden, 2009, pp. 1-12.
477 Morford JL, Emerson SR, Breckel EJ, Kim SH. Diagenesis of oxyanions (V, U, Re, and Mo) in pore
478 waters and sediments from a continental margin. Geochimica et Cosmochimica Acta 2005; 69:
479 5021-5032.
480 Nameroff TJ, Balistrieri LS, Murray JW. Suboxic trace metal geochemistry in the Eastern Tropical
481 North Pacific. Geochimica et Cosmochimica Acta 2002; 66: 1139-1158.
482 Parkhurst DL, Appelo CAJ. Description of input and examples for PHREEQC version 3—A computer
483 program for speciation, batch-reaction, one-dimensional transport, and inverse geochemical
484 calculations: U.S. Geological Survey Techniques and Methods, book 6, chap. A43, 497 p.,
485 2013.
486 Sørensen J. Reduction of Ferric Iron in Anaerobic, Marine Sediment and Interaction with Reduction of
487 Nitrate and Sulfate. Applied and Environmental Microbiology 1982; 43: 319-324.

488 Stookey LL. Ferrozine---a new spectrophotometric reagent for iron. Analytical Chemistry 1970; 42:
489 779-781.
490 Stumm W, Sulzberger B. The cycling of iron in natural environments: Considerations based on
491 laboratory studies of heterogeneous redox processes. Geochimica et Cosmochimica Acta 1992;
492 56: 3233-3257.
493 Sullivan P, Yelton J. An evaluation of trace element release associated with acid mine drainage.
494 Environmental Geology and Water Sciences 1988; 12: 181-186.
495 Tabaksblat LS. Specific Features in the Formation of the Mine Water Microelement Composition during
496 Ore Mining. Water Resources 2002; 29: 333-345.
497 Taylor, BE, Wheeler MC, Darrell KN. Stable isotope geochemistry of acid mine drainage: Experimental
498 oxidation of pyrite. Geochimica et Cosmochimica Acta 1984; 48: 2669-2678.
499 Van Hille RP, Boshoff GA, Rose PD, Duncan JR. A continuous process for the biological treatment of
500 heavy metal contaminated acid mine water. Resources, Conservation and Recycling 1999; 27:
501 157-167.
502 Wildeman TR, Ranville JR, Lee BT. Assessment of waters and sediments impacted by acid rock
503 drainage at the Young Dong coal mine site, South Korea, Final Report-Part A. Colorado School
504 of Mines, 2008.
505 Woo K, Lee J, Ji W, Khim J. Assessment of waters and sediments impacted by drainage at the Young
506 Dong coal mine site, South Korea. Environmental Science and Pollution Research 2012; 19:
507 19-30.
508 Yu J-Y. Precipitation of Fe and Al compounds from the acid mine waters in the dogyae area, Korea: A
509 qualitative measure of equilibrium modeling applicability and neutralization capacity?
510 Aquatic Geochemistry 1996; 2: 81-105.
511 Yu J-Y, Coleman M. Isotopic compositions of dissolved sulfur in acid mine drainages. Journal of the
512 Geological Society of Korea 2000; 36: 1-10.
513 Yu J-Y, Heo B. Dilution and removal of dissolved metals from acid mine drainage along Imgok Creek,

514 Korea. Applied Geochemistry 2001; 16: 1041-1053.
515 Yu J-Y, Heo B, Choi I-K, Cho J-P, Chang H-W. Apparent solubilities of schwertmannite and ferrihydrite
516 in natural stream waters polluted by mine drainage. Geochimica et Cosmochimica Acta 1999;
517 63: 3407-3416.
518 Yu J-Y. A mass balance approach to estimate the dilution and removal of the pollutants in stream water
519 polluted by acid mine drainage. Environmental Geology 1998; 36: 271-276.
520
521
522

Figure Captions

Figure 1. Study area and sampling points. Color coding indicates each water system; leachates from rock piles (sky blue), Young Dong (YD) stream (red), stream II (green), upstream of Imgok Creek (IC) (dark blue), and downstream of Imgok Creek (yellow). The numbers in each photo indicate the sampling point. Photos were taken in August 2011.

Figure 2. Spatial distribution of pH, conductivity, $acidity_{computed}$, and sulfate in Young Dong (YD) stream and downstream of Imgok Creek (IC). Closed and open symbols designate August 2011 and October 2011 samples, respectively.

Figure 3. Spatial distribution of Fe, Mn, Mg, Ca, Sr, Li, Co, Ni, Zn, and Pb (A), Al and Cu (B), Na and K (C) in Young Dong (YD) stream and downstream of Imgok Creek (IC). Closed and open symbols designate August 2011 and October 2011 samples, respectively.

Figure 4. Comparison of elemental concentrations (mg L^{-1}) of this study (n = 12) with past studies reported in Young Dong (YD) stream. 1) Woo et al., 2012 (n =6); 2) Lee et al., 2012 (n = 2); 3) Yu and Heo, 2001 (n =5); 4) Chon et al., 1999 (n = 7). The dotted lines indicate the time of limestone addition in 1999.

Figure 5. Comparison of elemental concentrations (mg L^{-1}) of this study (n = 10) with past studies reported in Imgok Creek (IC). 1) Woo et al., 2012 (n = 12); 2) Lee et al., 2012 (n = 2); 3) Yu and Heo, 2001 (n = 21); 4) Chon et al., 1999 (n = 11). The dotted lines indicate the time of limestone addition in 1999.

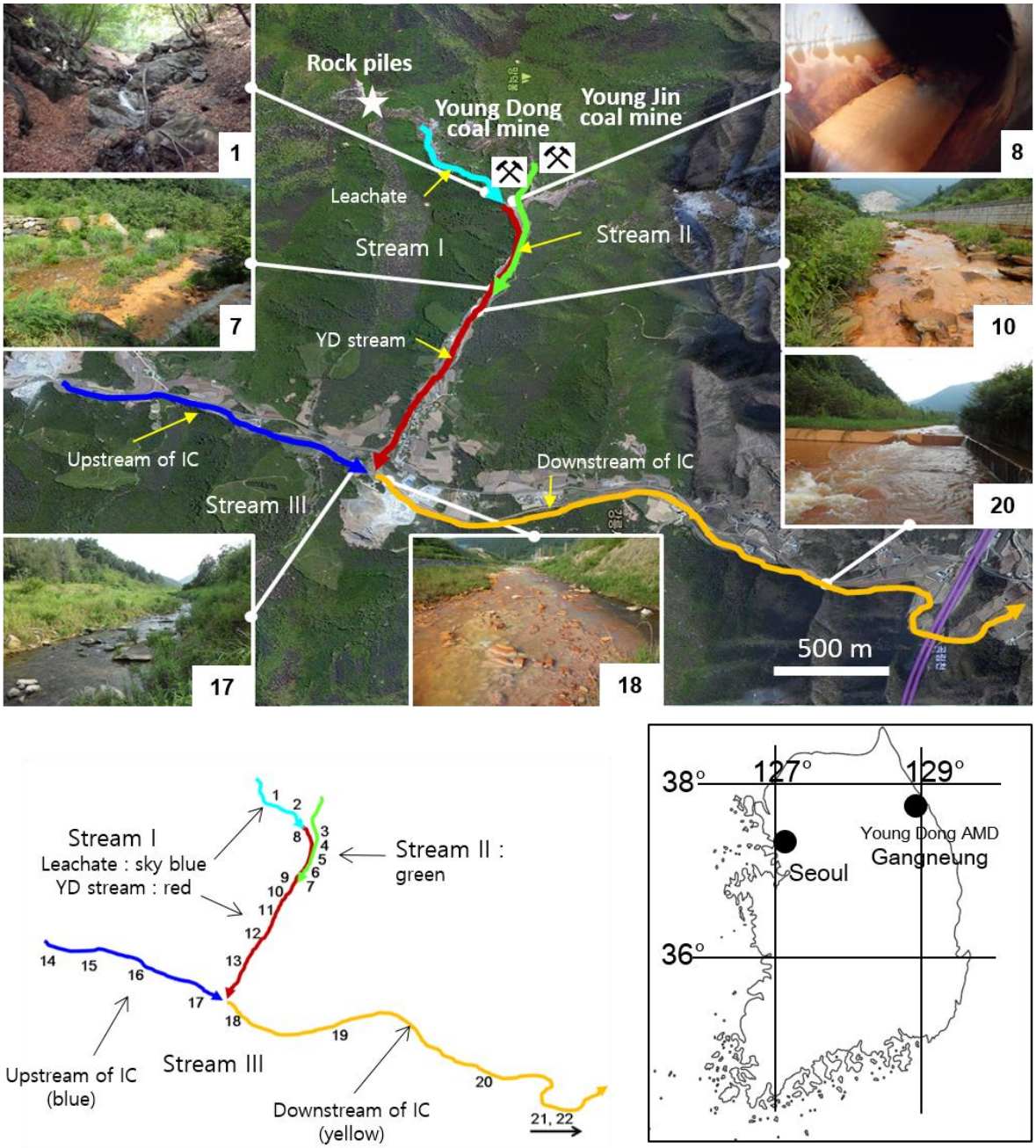

549

550

551 Fig. 1 Study area and sampling points

552

553

554

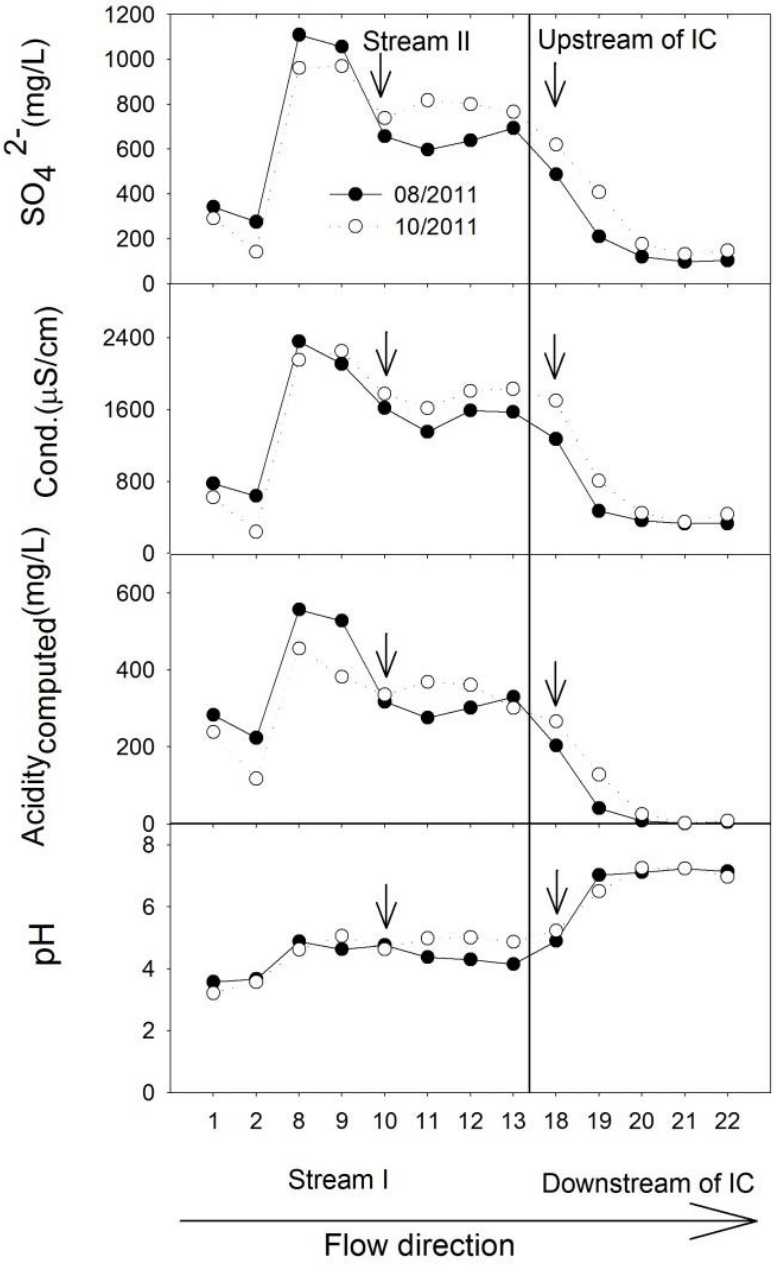

555

556

557 Fig. 2. Spatial distribution of pH, conductivity, acidity$_{computed}$, and sulfate in Young Dong (YD) stream

558 and downstream of Imgok Creek (IC).

559

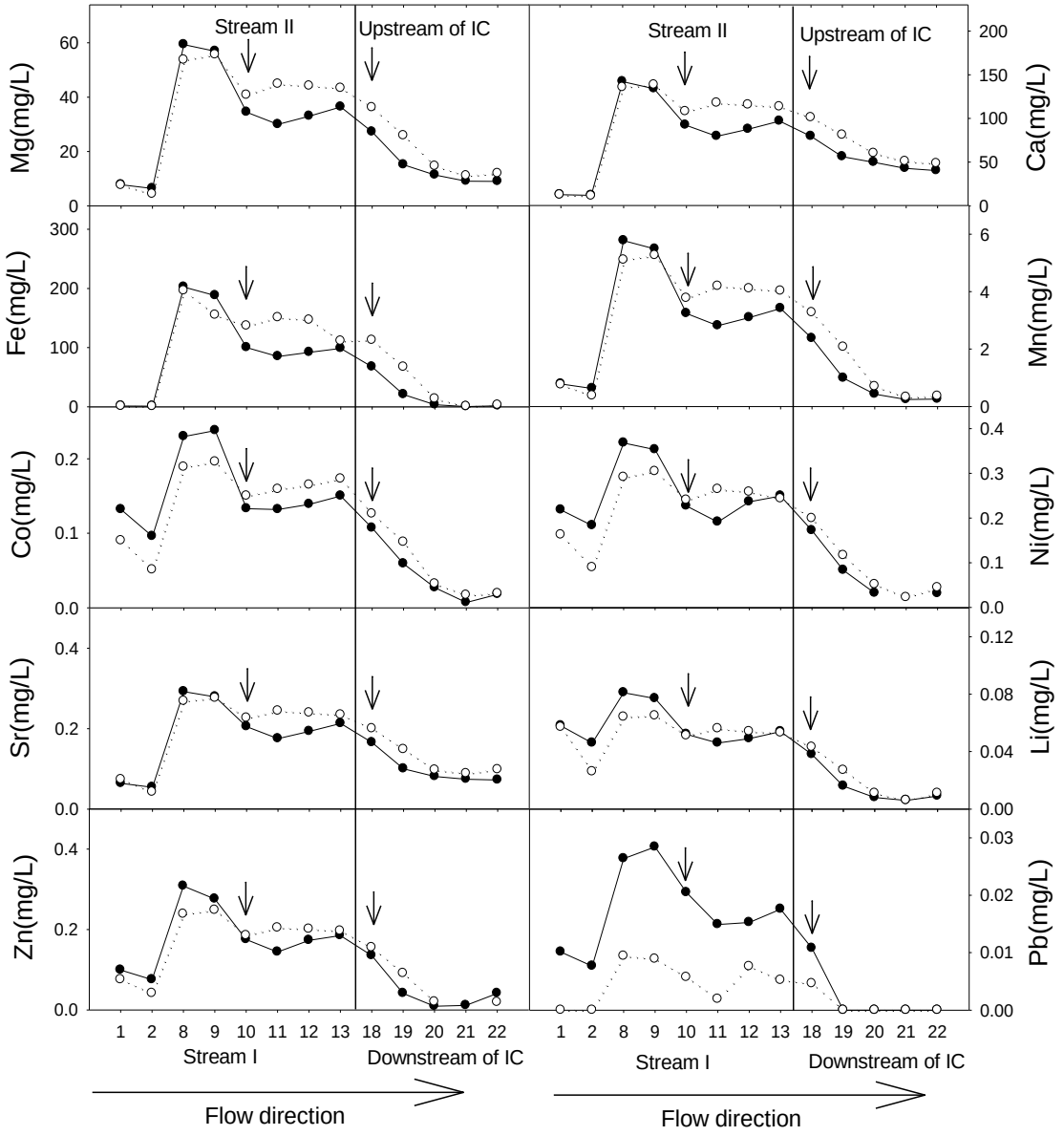

560

561

562 Fig. 3A. Spatial distribution of Fe, Mn, Mg, Ca, Sr, Li, Co, Ni, Zn, and Pb in Young Dong (YD) stream

563 and downstream of Imgok Creek (IC)

564

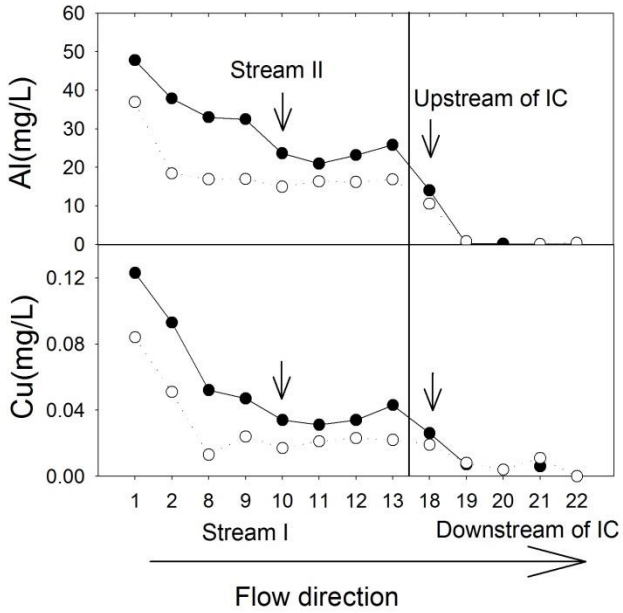

Fig. 3B. Spatial distribution of Al and Cu in Young Dong (YD) stream and downstream of Imgok Creek (IC)

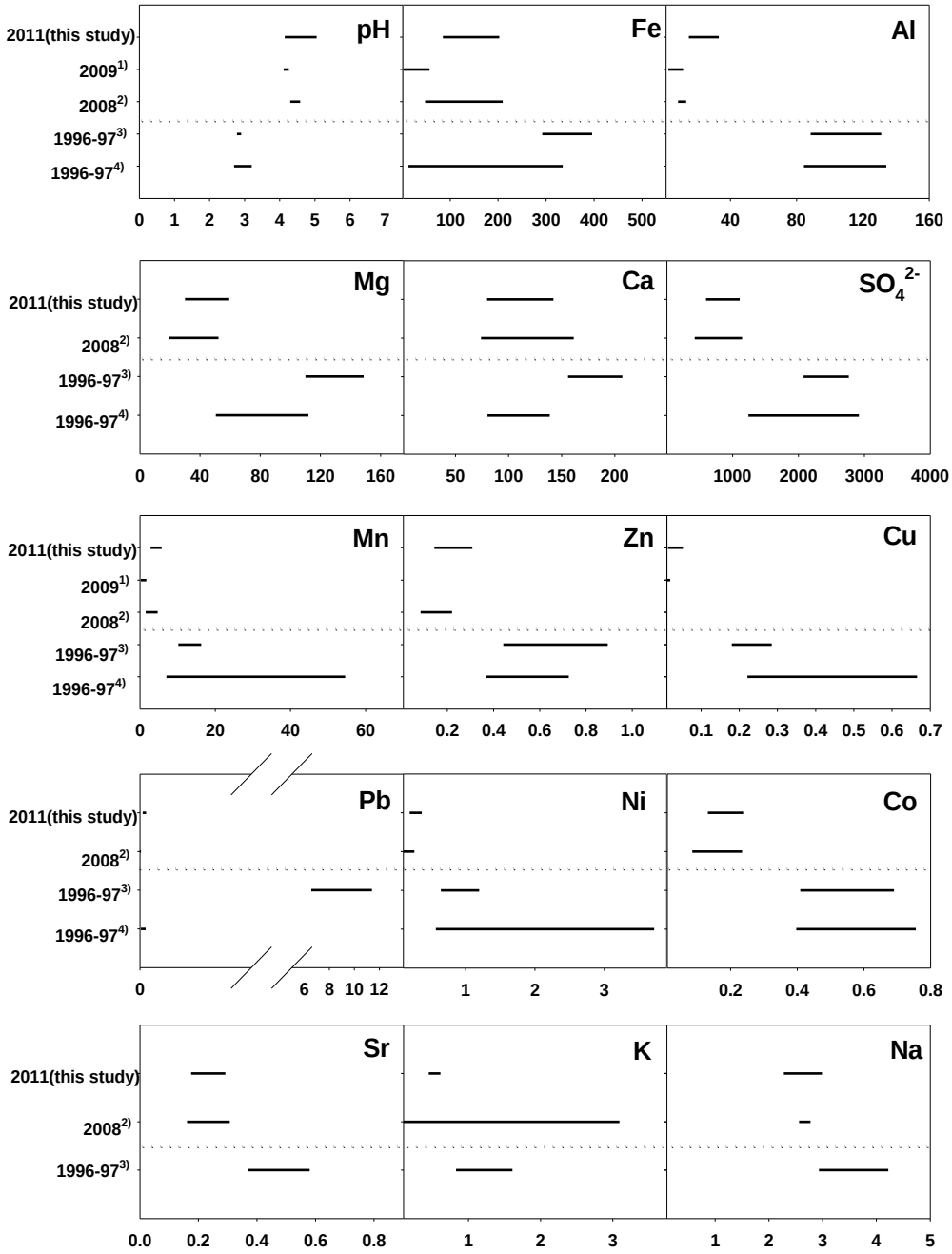

581

582 Fig. 4. Comparison of elemental concentrations (mg L^{-1}) of this study (n = 12) with past studies reported

583 in Young Dong (YD) stream

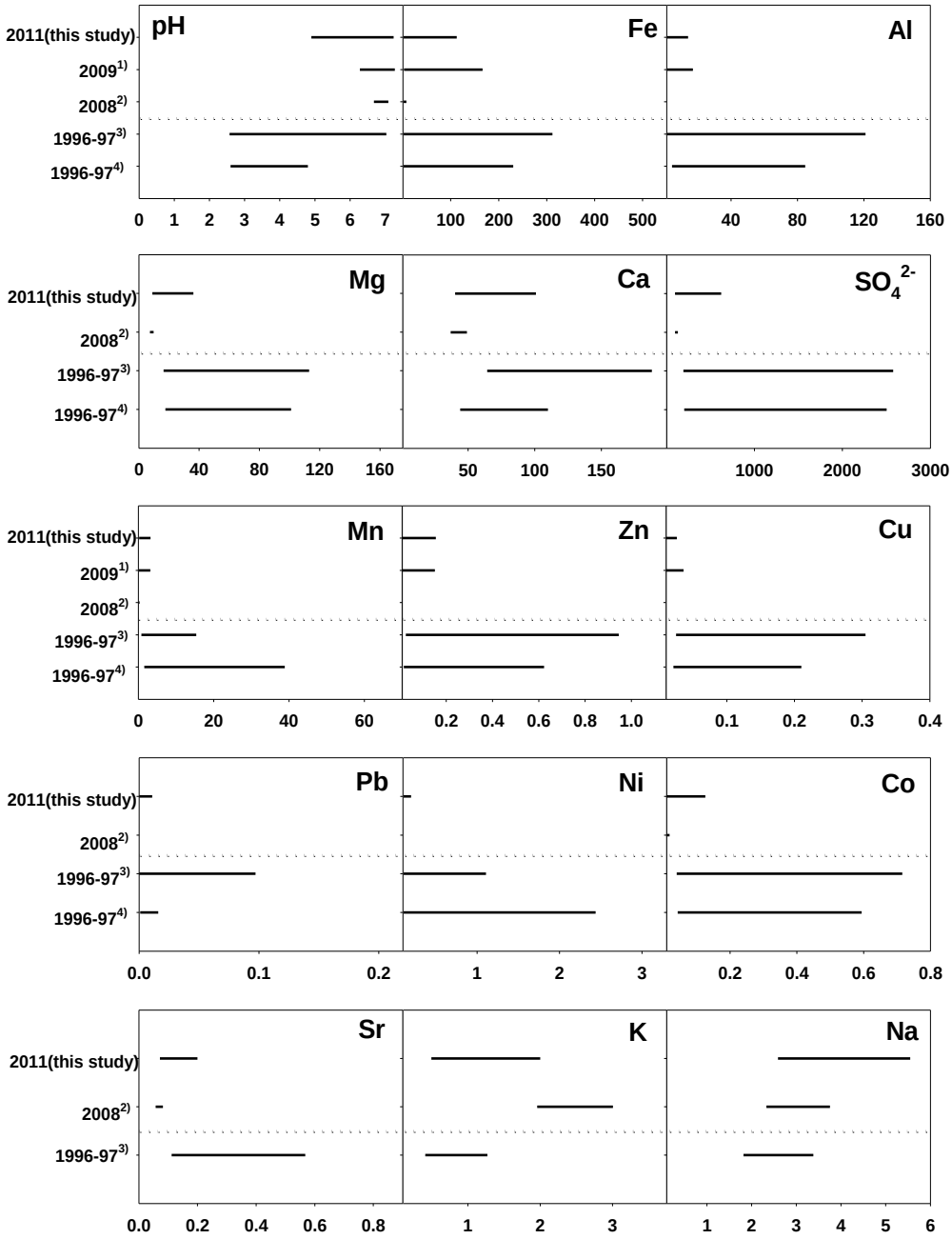

584

585 Fig. 5. Comparison of elemental concentrations (mg L^{-1}) of this study (n = 10) with past studies reported

586 in Imgok Creek (IC)

Table 1 General properties of each stream where water samples were collected

Water systems		Station no.	Properties*
Stream I	Leachates from rock piles	1, 2	Low pH, Fe, and sulfate / high Al / no precipitates
	Young Dong (YD) Stream	8, 9, 10, 11, 12, 13	Low pH/ high Fe and sulfate / Yellow brownish precipitates
Stream II	Young Jin Stream	3, 4, 5, 6, 7	Low pH, Fe, sulfate, and Al / Yellow brownish precipitates
Stream III	Upstream of Imgok Creek (IC)	14, 15, 16, 17	High pH/ low Fe, sulfate, and Al / no precipitates
	Downstream of Imgok Creek (IC)	18, 19, 20, 21, 22	High pH/ low Fe, sulfate, and Al / Yellow brownish and whitish precipitates

* The properties were described based on the relative values of the general water quality and ion concentrations as shown in Table S2

Supporting Information for

Water quality changes in acid mine drainage streams in Gangneung, Korea, 10 years after treatment with limestone

Moo Joon Shim[1], Byung Young Choi[2], Giehyeon Lee[3], Yun Ho Hwang[1],

Jung-Seok Yang[1], Edward J. O'Loughlin[4], and Man Jae Kwon[1*]

[1] Korea Institute of Science and Technology, Gangneung, KOREA

[2] Korea Institute of Geoscience and Mineral Resources, Daejeon, KOREA

[3] Earth System Sciences, Yonsei University, Seoul, KOREA

[4] Biosciences Division, Argonne National Laboratory, Argonne, USA

*Corresponding Author: Korea Institute of Science and Technology, Gangneung, KOREA, 679 Saimdangro, Gangneung, Gangwon-do, 210-340, Korea, Phone: +82-33-650-3705; Fax: +82-33-650-3729; mkwon@kist.re.kr

A manuscript submitted to *Journal of Geochemical Exploration*

May, 2015

10 pages, 3 Figures, 4 Tables

Supporting Information provides additional results for XRF and XRD analysis and saturation indices

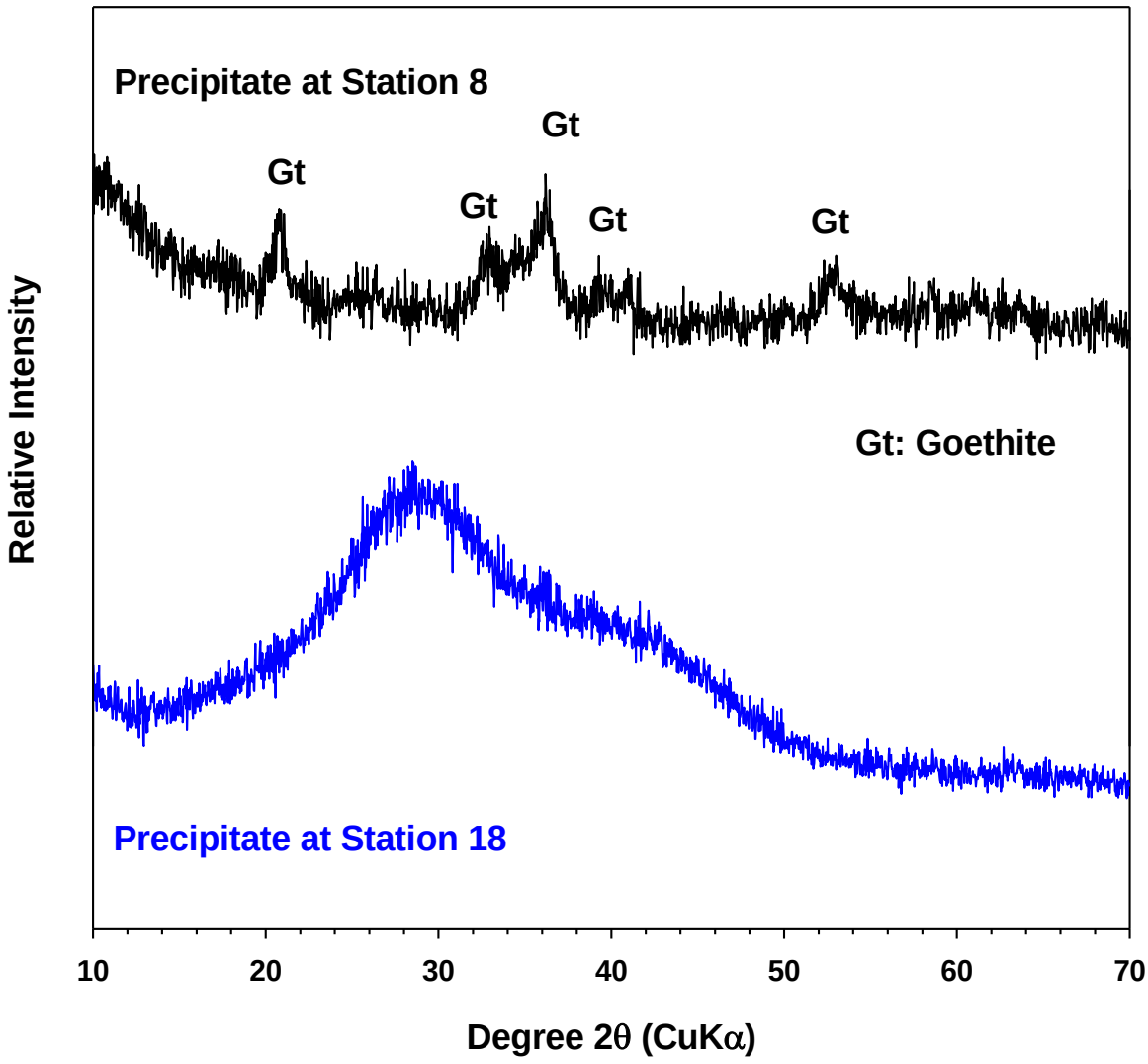

Figure S1. XRD patterns of the solid precipitates collected from the station 8 and 18. The XRD pattern of the sample from the station 8 was similar to that of typical goethite (JCPDS 29-0713)

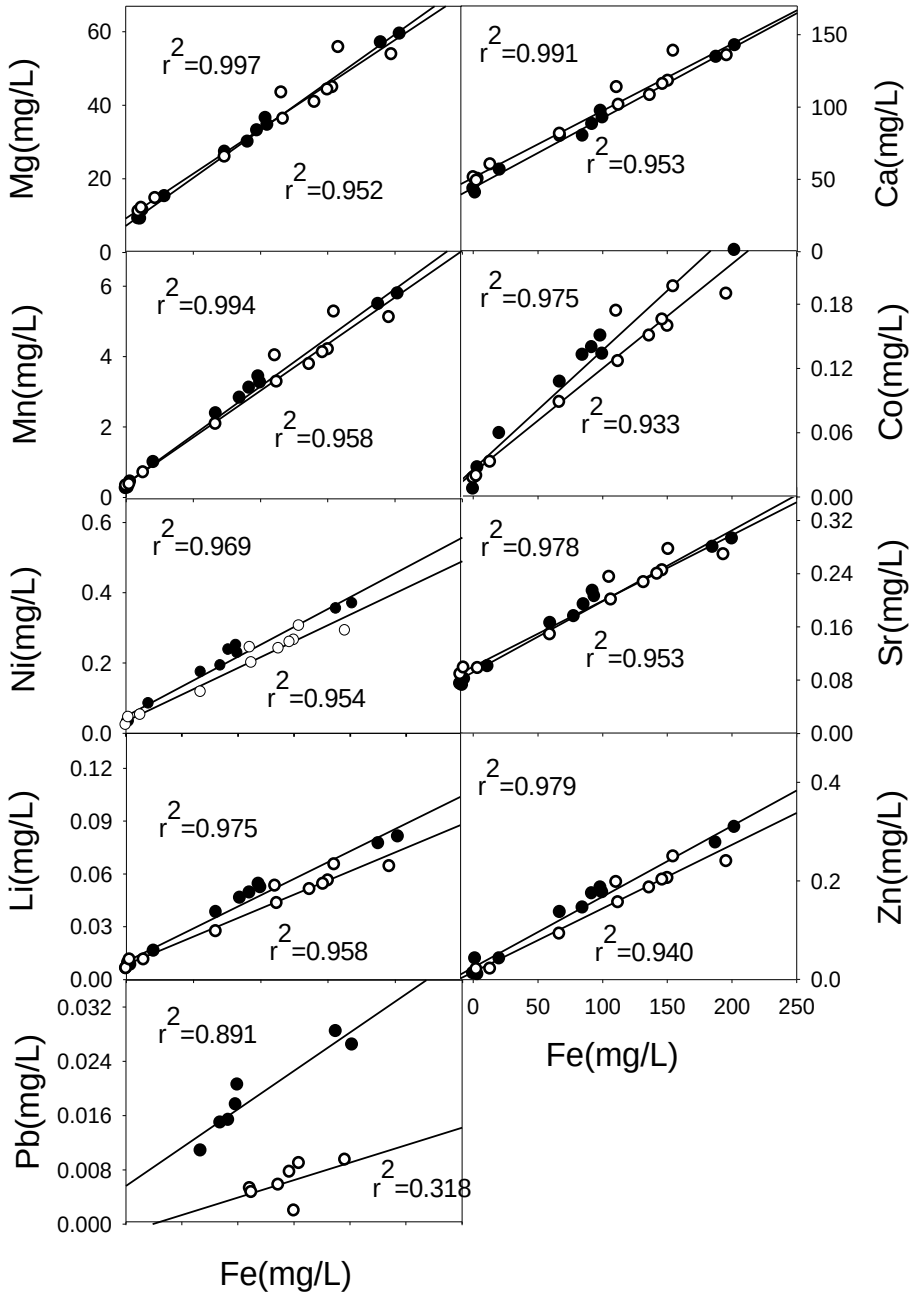

Figure S2. The relationship between Fe and Mn, Mg, Ca, Sr, Li, Co, Ni, Zn, and Pb. The data from leachates, stream II, and upstream of Imgok Creek were not plotted. Closed and open symbols designate August 2011 and October 2011 samples, respectively

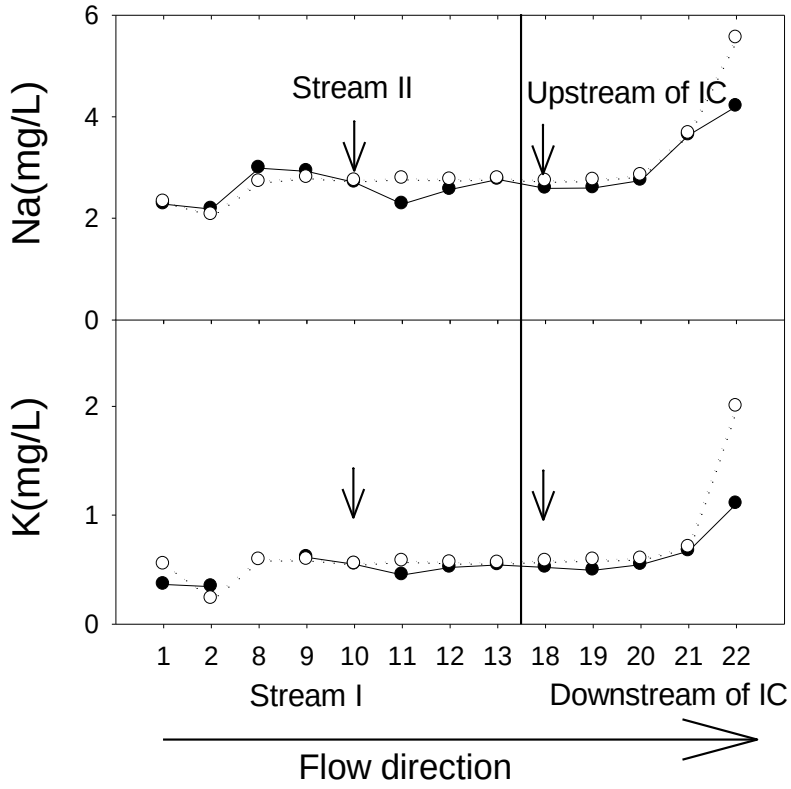

Figure S3. Spatial distribution of Na and K in Young Dong (YD) stream and downstream of Imgok Creek (IC). Closed and open symbols designate August 2011 and October 2011 samples, respectively.

The spatial distributions of K and Na were largely different compared to the other elements analyzed in this study (Fig. 3C). Like the first group of elements, K and Na levels were relatively low in leachates (stations 1 and 2), but slightly increased at station 8 where the YD AMD directly came out of the adit. Before the convergence of YD stream with IC, concentrations of K and Na remained constant (Fig. 3C). Unlike the other elements, K and Na increased in downstream waters of IC. These results suggest that agricultural and livestock farming activities along IC might have led to higher K and Na concentrations in downstream waters of IC. Sodium nitrate ($NaNO_3$) and potassium nitrate (KNO_3) are sources of Na and K in many fertilizers (Rasiah et al., 1992) and livestock wastewater (Cho et al., 2000). Therefore,

K and Na may have entered into IC as runoff from rice paddies and vegetable fields and wastewater from livestock staples located near IC.

References

Cho J-C, Cho HB, Kim S-J. Heavy contamination of a subsurface aquifer and a stream by livestock wastewater in a stock farming area, Wonju, Korea. Environmental Pollution 2000; 109: 137-146.

Rasiah V, Voroney RP, Kachanoski RG. Biodegradation of an oily waste as influenced by nitrogen forms and sources. Water, Air, and Soil Pollution 1992; 65: 143-151.

US Environmental Protection Agency. National Primary Drinking Water Regulations. EPA 816-F-02-013, Washington, DC. 2009

Table S1. Saturation indices of waters with respect to minerals. Thermodynamic data were extracted from THERMODDEM (http://thermoddem.brgm.fr)

Water systems	Station	pH	Saturation indices									
			Basaluminite	Boehmite	Gibbsite	Ferrihydrite	Goethite	Schwertmannite	Calcite	Dolomite	Gypsum	Magnesioferrite
Leachates from rock piles	1	3.4	-5.6	-0.9	-1.1	-7.2	-4.2	-49.1	-	-	-20	-23.9
	2	3.6	-3.8	-0.3	-0.5	-6.7	-3.6	-45.3	-	-	-2.1	-22.4
Young Jin Stream	3	3.9	-2.5	0.1	0.0	-6.1	-3.0	-41.0	-	-	-1.4	-20.4
	4	4.0	-0.3	0.7	0.6	-5.7	-2.7	-38.1	-	-	-1.2	-19.2
	5	4.2	1.4	1.2	1.1	-5.0	-2.0	-33.4	-	-	-1.5	-17.6
	6	4.6	4.6	2.2	2.1	-4.1	-1.1	-26.8	-	-	-1.4	-15.1
	7	4.7	5.7	2.6	2.5	-2.8	0.2	-16.8	-	-	-1.5	-12.3
Young Dong Stream	8	4.8	6.0	2.5	2.4	-1.0	2.0	-1.7	-	-	-0.7	-8.0
	9	4.8	6.8	2.8	2.7	-0.8	2.2	-0.2	-	-	-0.7	-7.4
	10	4.7	5.3	2.3	2.2	-1.3	1.7	-4.4	-	-	-0.9	-8.9
	11	4.7	5.0	2.3	2.2	-1.4	1.6	-4.9	-	-	-0.9	-9.1
	12	4.7	4.9	2.2	2.1	-1.5	1.6	-5.3	-	-	-0.9	-9.2
	13	4.5	3.6	1.8	1.7	-2.0	1.1	-9.2	-	-	-0.9	-10.6
Downstream of Imgok Creek	18	5.1	8.0	3.2	3.1	-0.3	2.7	2.8	-	-	-1.0	-6.2
	19	6.8	5.7	3.6	3.4	4.5	7.5	37.7	-1.6	-3.3	-1.2	6.7
	20	7.2	1.0	2.6	2.5	4.9	7.9	39.9	-0.9	-2.1	-1.5	8.2
	21	7.2	-0.3	3.4	2.3	3.5	6.5	28.7	-0.9	-2.0	-1.6	5.5
	22	7.1	2.9	3.1	3.0	4.0	7.1	33.3	-1.3	-2.8	-1.6	6.2

Table S2. General water quality and concentrations of major and trace elements

Date	Stn.	pH	EC	SO_4^{2-}	NO_3^-	Cl^-	Alk.	$Acidity_{comp}$	Metals and major ions (mg/L)														
			(uS/cm)	(mg/L)	(mg/L)	(mg/L)	(mg/L)	(mg/L)	Al	K	Na	Ni	Cu	Pb	Sr	Ca	Co	Fe	Fe^{2+}	Mg	Mn	Zn	Li
08/2011	**1**	3.6	778	342	4.0	5.5	NA	282	47.7	0.4	2.3	0.22	0.12	0.01	0.06	12.7	0.13	1.3	1	7.8	0.79	0.10	0.06
	2	3.7	637	275	2.4	NA	NA	224	37.8	0.3	2.2	0.18	0.09	0.01	0.05	12.0	0.1	0.9	ND	6.4	0.63	0.08	0.05
	3	4.3	554	274	10.0	5.0	NA	90	15.2	7.9	2.6	0.16	0.04	ND	0.18	55.3	0.07	0.9	ND	15.1	0.97	0.16	0.04
	4	3.8	648	306	25.5	5.1	NA	166	28.2	1.2	2.4	0.17	0.05	0.01	0.13	40.8	0.09	0.2	ND	12.1	0.87	0.09	0.05
	5	4.2	586	256	20.7	5.8	NA	114	19.5	0.5	2.3	0.14	0.03	0.01	0.14	42.2	0.08	0.7	ND	12.0	0.81	0.08	0.04
	6	4.4	617	250	14.4	5.9	NA	103	17.9	0.5	2.5	0.12	0.04	0.01	0.16	47.0	0.07	0.4	ND	11.1	0.73	0.08	0.03
	7	4.6	448	219	11.4	5.5	NA	95	16.0	0.4	2.4	0.11	0.04	0.01	0.13	40.2	0.07	1.9	ND	9.2	0.68	0.07	0.03
	8	4.9	2358	1109	10.8	6.1	NA	557	33.0	NA	3.0	0.37	0.05	0.03	0.29	142.0	0.23	202.0	204	59.3	5.77	0.31	0.08
	9	4.6	2107	1055	17.1	5.1	NA	528	32.5	0.6	2.9	0.35	0.05	0.03	0.28	134.0	0.24	188.0	187	56.9	5.48	0.28	0.08
	10	4.8	1619	657	10.5	5.6	NA	317	23.6	0.6	2.7	0.23	0.03	0.02	0.21	92.3	0.13	100.0	99	34.5	3.24	0.18	0.05
	11	4.4	1351	597	19.5	5.7	NA	276	21.0	0.5	2.3	0.19	0.03	0.01	0.18	79.7	0.13	84.8	104	29.9	2.81	0.14	0.05
	12	4.3	1590	639	17.4	5.2	NA	302	23.2	0.5	2.6	0.24	0.03	0.02	0.19	87.7	0.14	92.0	98	33.0	3.09	0.17	0.05
	13	4.1	1576	693	15.3	5.7	NA	330	25.8	0.5	2.8	0.25	0.04	0.02	0.21	96.8	0.15	98.7	93	36.4	3.42	0.19	0.05
	14	6.5	286	18	20.7	5.5	123	1	ND	0.5	2.5	ND	0.01	ND	0.07	47.2	ND	0.3	ND	7.0	0.00	0.02	ND
	15	6.4	95.8	19	17.1	5.4	123	0	ND	0.5	2.5	ND	0.01	ND	0.07	47.5	ND	0.2	ND	7.2	0.00	ND	ND
	16	7.9	173	56	16.8	6.0	153	0	ND	2.1	3.2	ND	0.01	0.01	0.15	41.9	ND	0.1	ND	15.6	0.00	ND	0.001
	17	8.1	393	93	24.6	5.5	142	0	ND	2.2	3.1	ND	0.01	0.01	0.21	79.7	ND	0.1	ND	18.8	0.00	0.01	0.001
	18	4.9	1271	487	15.9	5.5	NA	203	14.0	0.5	2.6	0.17	0.03	0.01	0.17	79.6	0.11	67.2	69	27.2	2.37	0.14	0.04
	19	7.0	470	211	10.5	5.9	30	40	0.3	0.5	2.6	0.08	0.01	ND	0.1	56.3	0.06	20.6	20	15.1	0.99	0.04	0.02
	20	7.1	364	119	19.2	6.0	47	8	0.1	0.6	2.8	0.03	ND	ND	0.08	49.8	0.03	3.4	ND	11.4	0.43	0.01	0.01
	21	7.2	329	97	28.2	6.7	50	1	0.1	0.7	3.6	ND	0.01	ND	0.07	43.0	0.01	0.2	ND	9.1	0.24	0.01	0.01
	22	7.1	331	103	13.5	8.1	33	4	0.2	1.1	4.2	0.03	ND	ND	0.07	40.3	0.02	1.7	ND	9.0	0.26	0.04	0.01

Continued

Date	Stn.	pH	EC	SO_4^{2-}	NO_3^-	Cl^-	Alk.	$Acidity_{comp}$	Metals and major ions (mg/L)														
			(uS/cm)	(mg/L)	(mg/L)	(mg/L)	(mg/L)	(mg/L)	Al	K	Na	Ni	Cu	Pb	Sr	Ca	Co	Fe	Fe^{2+}	Mg	Mn	Zn	Li
10/2011	**1**	3.2	623	291	NA	5.1	NA	239	36.9	0.6	2.3	0.16	0.08	ND	0.07	12.5	0.09	0.8	ND	7.5	0.76	0.08	0.06
	2	3.6	237	142	NA	5.4	NA	117	18.4	0.2	2.1	0.09	0.05	ND	0.04	11.3	0.05	0.5	ND	4.3	0.37	0.04	0.03
	3	3.4	448	278	NA	4.9	NA	123	18.5	0.5	2.7	0.12	0.03	0.01	0.17	50.2	0.07	0.2	ND	12.8	0.83	0.07	0.03
	4	4.2	853	419	NA	5.3	NA	130	22.1	0.8	2.9	0.21	0.05	ND	0.31	84.5	0.12	0.7	ND	23.7	1.70	0.14	0.05
	5	4.3	394	262	NA	5.2	NA	110	19.1	0.5	2.5	0.10	0.03	ND	0.15	44.1	0.06	0.2	ND	11.6	0.77	0.07	0.03
	6	4.8	469	228	NA	6.0	NA	67	11.7	0.4	2.6	0.08	0.02	ND	0.15	51.5	0.05	0.2	ND	9.9	0.56	0.05	0.02
	7	4.9	453	225	NA	5.2	NA	73	11.9	0.4	2.6	0.11	0.03	0.01	0.14	49.6	0.06	2.6	ND	9.9	0.60	0.05	0.02
	8	4.6	2153	961	NA	5.4	NA	456	16.9	0.6	2.7	0.29	0.01	0.01	0.27	135.0	0.19	196.0	190	53.7	5.10	0.24	0.06
	9	5.1	2252	968	NA	5.2	NA	382	17	0.6	2.8	0.30	0.02	0.01	0.28	138.0	0.20	155.0	183	55.6	5.26	0.25	0.07
	10	4.6	1777	738	NA	5.7	NA	336	14.9	0.6	2.7	0.24	0.02	0.01	0.23	108.0	0.15	137.0	124	40.7	3.77	0.19	0.05
	11	5.0	1616	817	NA	5.4	NA	369	16.4	0.6	2.8	0.26	0.02	0.00	0.24	118.0	0.16	151.0	135	44.8	4.19	0.20	0.06
	12	5.0	1806	799	NA	5.7	NA	361	16.2	0.6	2.8	0.26	0.02	0.01	0.24	115.0	0.17	147.0	132	44.1	4.10	0.20	0.05
	13	4.9	1830	765	NA	5.5	NA	301	16.9	0.6	2.8	0.24	0.02	0.01	0.23	113.0	0.17	111.0	129	43.3	4.02	0.20	0.05
	14	6.8	299	16	NA	5.7	NA	1	ND	0.6	2.6	ND	ND	ND	0.07	47.8	ND	0.4	ND	6.4	ND	ND	ND
	15	7.6	207	16	NA	5.9	NA	0	ND	0.6	2.6	ND	0.01	ND	0.07	48.5	ND	0.2	NA	6.5	ND	ND	ND
	16	NA	NA	NA	NA	NA	NA	NA	NA	NA	NA	NA	NA	NA	NA	NA	NA	NA	NA	NA	NA	NA	NA
	17	NA	NA	NA	NA	NA	NA	NA	NA	NA	NA	NA	NA	NA	NA	NA	NA	NA	NA	NA	NA	NA	NA
	18	5.2	1699	620	NA	5.0	NA	266	10.5	0.6	2.7	0.20	0.02	0.01	0.20	101.0	0.13	112.0	105	36.2	3.27	0.16	0.04
	19	6.5	805	408	NA	5.0	NA	128	0.8	0.6	2.8	0.12	0.01	ND	0.15	81.1	0.09	67.0	64	25.8	2.07	0.09	0.03
	20	7.3	446	175	NA	5.9	NA	25	ND	0.6	2.8	0.05	0.00	ND	0.10	59.9	0.03	13.3	12	14.6	0.69	0.02	0.01
	21	7.2	347	131	NA	6.1	NA	2	0.1	0.7	3.7	0.02	0.01	ND	0.09	50.8	0.02	0.4	ND	11.0	0.32	ND	0.01
	22	7.0	434	147	NA	8.2	NA	8	0.4	2.0	5.6	0.04	ND	ND	0.10	48.5	0.02	2.8	2	11.9	0.36	0.02	0.01

ND: Not detected
NA: Not available

Table S3. X-ray fluorescence spectroscopy (XRF) analysis of major elements in the precipitates collected from the bottom of stream waters

Formula	Concentrations (%)	
	Stn. 8	**Stn. 18**
Al_2O_3	2.38	58.40
Fe_2O_3	86.51	8.62
SO_3	10.62	30.55
SiO_2	0.38	2.22
CaO	0.05	0.10
Cl	0.02	0.03
K_2O	0.00	0.03
P_2O_5	0.00	0.03
TiO_2	0.00	0.02
Cr_2O_3	0.01	0.00
CuO	0.01	0.00
MnO	0.01	0.00
sum	100.00	100.00

Table S4. List of contaminants measured in this study and their maximum contaminant levels (MCLs)(US EPA, 2009). ▲: value exceeding the MCL, ▽: value not exceeding or within the MCL

	Contaminant	Maximum Contaminant Level (mg L-1)	YD stream (station 8-13)	Downstream IC (station 19-22)
National Primary Drinking Water Regulation	Copper	1.3	▽	▽
	Lead	0.015	▲	▽
	Nitrate (measured as N)	10	▽	▽
National Secondary Drinking Water Regulation	Aluminum	0.05-0.2	▲	▽
	Chloride	250	▽	▽
	Iron	0.3	▲	▲
	Manganese	0.05	▲	▲
	pH	6.5-8.5	▲	▽
	Sulfate	250	▲	▽
	Zinc	5	▽	▽